arXiv:1204.5445v1 [physics.geo-ph] 24 Apr 2012

A recent bifurcation in Arctic sea-ice cover

Valerie N. Livina[1] and Timothy M. Lenton[2]

[1] *School of Environmental Sciences, University of East Anglia, Norwich, UK*

[2] *College of Life and Environmental Sciences, University of Exeter, UK*

June 20, 2013

Abstract

There is ongoing debate over whether Arctic sea-ice has already passed a 'tipping point', or whether it will do so in future, with several recent studies arguing that the loss of summer sea ice does not involve a bifurcation because it is highly reversible in models. Recently developed methods can detect and sometimes forewarn of bifurcations in time-series data, hence we applied them to satellite data for Arctic sea-ice cover. Here we show that a new low ice cover state has appeared from 2007 onwards, which is distinct from the normal state of seasonal sea ice variation, suggesting a bifurcation has occurred from one attractor to two. There was no robust early warning signal of critical slowing down prior to this bifurcation, consistent with it representing the appearance of a new ice cover state rather than the loss of stability of the existing state. The new low ice cover state has been sampled predominantly in summer-autumn and seasonal forcing combined with internal climate variability are likely responsible for triggering recent transitions between the two ice cover states. However, all early warning indicators show destabilization of the summer-autumn sea-ice since 2007. This suggests the new low ice cover state may be a transient feature and further abrupt changes in summer-autumn Arctic sea-ice cover could lie ahead; either reversion to the normal state or a yet larger ice loss.

Arctic sea-ice has experienced striking reductions in areal coverage [1, 2], especially in recent summers, with 2007-2011 having the five lowest ice cover minima in the satellite record (Figure 1). Observations have fallen below IPCC model projections [1], despite the models having been in agreement with the observations in the 1970s. Summer ice cover is forecast to disappear later this century [3], but the nature of the underlying transition is debated [4, 5, 6, 7, 8, 9]. Arctic sea-ice has been identified as a potential tipping element in the Earth's climate system [4], and at least one study suggests it has already passed a 'tipping point' [5]. In the future, some models forecast abrupt ice loss events [6], on the way to a seasonally ice-free Arctic. These may qualify as passing tipping points following the definition in [4], which includes both reversible and irreversible transitions. However, most recent papers address whether summer sea-ice loss will involve an irreversible (e.g. saddle-node/fold)

bifurcation, and they find instead that in models the loss of summer sea-ice cover is highly reversible [6, 7, 8, 9]. Abrupt ice loss events are then attributed to the loss of year-round sea-ice in the Arctic making the remaining ice more vulnerable to summer melt, and prone to larger fluctuations in area coverage [10]. One exception is a recent model [11] showing that positive feedbacks involving clouds can create multiple stable states for seasonal ice cover and bifurcations between them.

Here we try to resolve whether the Arctic sea-ice is approaching, or has passed, a bifurcation point by applying methods of time-series analysis that can detect [12, 13] and in some cases forewarn [14, 15, 16, 17] of bifurcations. We analyse the satellite-derived daily record of sea-ice area from 1979 to present (Figure 1a), and repeat the analysis on sea-ice extent data [18] (Supplementary Figure 1). For our analysis, the mean seasonal cycle (Figure 1b) is removed from the data, because there is a very strong seasonally-forced variation in sea-ice area, but we are interested in the behavior of fluctuations from this typical state of seasonal variation. The last five years have been characterized by an increase in the amplitude of seasonal sea-ice variation (Figure 1a), as the annual ice cover minimum dropped the order of $\sim 10^6$ km^2 more than the annual maximum in 2007 and the difference has been maintained since then (Figure 1c). This hints that a new attractor for summer-autumn sea-ice cover may have been sampled in the last 5 years.

1 Bifurcation detection

After removing the mean seasonal cycle, the remaining fluctuations in sea-ice area include some of order 10^6 km^2 (Figure 2a). The largest anomalies are in 1996 (maximum of the series) and 2007-2011 (minima). They typically occur in the summer-autumn, when the sea-ice area is at its lowest in the seasonal cycle. Given the size of sea-ice fluctuations during 2007-2011 (Figure 2a) and the pronounced drop in sea-ice minima relative to sea-ice maxima since 2007 (Figure 1c), we considered whether a new, lower sea ice cover state has started to appear.

To detect such a transition, we use a recently-developed [12, 13] and rigorously blind-tested [19] method of 'potential analysis' (see Methods). This assumes that a system is experiencing sufficient short-term stochastic variability (noise) that it is sampling all of its available states or attractors (given a sufficiently long time window). Then we take advantage of the fact that the stationary probability distribution of the resulting data is directly related to the shape of the underlying potential, which describes the number of underlying system states and their stability [13]. Thus, with a sufficiently long time window of data one can deduce the number of system states and their relative stability or instability. A test of the method on artificial data, generated from a model system in which the underlying potential bifurcates from one state to two, illustrates correct detection of the number of system states (Supplementary Figure 2). Detection is most reliable when the time window exceeds $\sim$400 data

points [13], which in the case of daily data corresponds to about 1.1 years.

On analyzing the sea-ice area data, over long time windows (here >1 year), we typically find a single sea-ice state, representing the normal seasonal cycle of variability (Figure 2b). Sometimes a second state is detected associated with e.g., the sea-ice maximum in 1996, but these changes are not found simultaneously and persistently across a wide range of window lengths. However, from 2007 onwards, a persistent switch to two states in sea-ice cover fluctuations is detected, across a wide range of window lengths up to >10 years (Figure 2b). The same switch is also detected in analysis of sea-ice extent data (Supplementary Figure 3).

The stability of the sea-ice state(s) can be reconstructed, in the form of potential curves for fixed intervals of the data (Figure 2c), with associated error estimates (on the coefficients of the polynomial function describing the potential [13]). The sea-ice is typically characterized by a single stable state. The interval 1996-9 (including the 1996 maximum anomaly) shows signs of a second high ice state that is degenerate (i.e. not fully stable). In 2000-3 there is a return to a single state. In 2004-7, which includes the record September 2007 sea-ice retreat, a low ice-cover state starts to appear. Then in 2008-11 the potential separates into two stable states, although the error range allows for one or the other of these to be degenerate. The potential curves are derived from histograms of the original data [13] (Figure 2d), which confirm a second mode appearing among a long tail of negative fluctuations during 2004-2007, followed by a separation of modes during 2008-2011. Thus, we argue that Arctic sea-ice recently passed a bifurcation point, which created a new lower ice cover state. Since then it has fluctuated between its normal state of seasonal variability and the new, lower ice cover state.

2 Early warnings?

Having detected a bifurcation in Arctic sea-ice cover we considered whether it was preceded (or followed) by any signals of destabilization. For a low-order dynamical system approaching a threshold where its current state becomes unstable, and it transitions to some other state, one can expect to see it become more sluggish in its response to small perturbations [14]. This can hold even for complex systems such as the sea-ice, because near to a bifurcation point their behavior reduces down to that of a low-order system (following the Center Manifold Theorem). This signal of 'critical slowing down' [14] is detectable as increasing autocorrelations in time series data, occurring over timescales capturing the decay of the major mode in the system [15], which is controlled by the leading eigenvalue. We looked for this early warning indicator in the form of rising lag-1 autocorrelation [15] (ACF-indicator), and through detrended fluctuation analysis (DFA-indicator) as a rising scaling exponent [16] (see Methods). We also monitored variance (calculated as standard deviation), because if a state is becoming less stable this can be characterized by its potential well getting shallower, causing increased variability over time (although this is not indepen-

dent of lag-1 autocorrelation [20]). Before applying these methods, we removed the overall quadratic downward trend in sea-ice area (and extent), because this can cause the indicators to rise (giving false positives). We also conducted a sensitivity analysis for the detected trends in the indicators, by varying the size of the sliding window in which they are calculated over 0.25-0.75 of the length of each data set.

We note that the bifurcation inferred (Figure 2, Supplementary Figure 3) represents the creation of a new ice cover state (in the fluctuations) rather than the total loss of stability of the existing ice cover state. Hence the existing ice cover state may not show any destabilization prior to the bifurcation. Sure enough, prior to 2007 there is no consistent early warning signal of destabilization (Figure 3c, e, g). The indicators all increased around the anomalous sea-ice maximum in 1996, but then they all declined toward 2007, consistent with our potential reconstruction (Figure 2c). The only early warning signal prior to 2007 is a rise in the DFA-indicator in analysis of sea ice extent (Supplementary Figure 4). Sensitivity analysis confirms this is the only robust increase across the three indicators and the two datasets, prior to 2007 (Supplementary Figure 5). Thus, there was no consistent early warning signal of critical slowing down before the bifurcation. Indeed the normal sea-ice state showed signs of increasing stability in the preceding decade.

The sea-ice retreat in 2007 caused abrupt increases in all the indicators, which have continued to rise since then (Figure 3c, e, g). Sensitivity analysis reveals a robust upward trend in the DFA-indicator across the whole dataset (Figure 3d), but no robust overall trend in the ACF-indicator or variance (Figure 3b, f). These results are reproduced in analysis of sea-ice extent data (Supplementary Figure 4). The rise in the DFA-indicator is consistent with the sea-ice having increasing 'memory' of its earlier states due to critical slowing down [16], and the somewhat different behavior of the ACF and DFA indicators could be explained by the different time scales used for their calculation. The ACF-indicator, based only on lag-1 autocorrelation (here from one day to the next), may be monitoring the behavior of fast decay modes unrelated to critical slowing down. The DFA-indicator in contrast is calculated on time scales up to 100 days, which should be long enough to capture the slowest recovery mode of the sea-ice.

We conclude that overall the indicators detect destabilization in 2007, which is ongoing, but do not forewarn of it.

Analysis of a much longer reconstruction of Arctic sea-ice extent since 1870 at annual resolution [21], shows a strong and robust upward trend in inter-annual variability (variance) of the sea-ice prior to recent retreats (Supplementary Figure 6), but no other early warning signals. Such increased variability of the sea-ice cover as it thins [10] could have encouraged recent transitions between ice cover states. This might support an alternative hypothesis that the low ice cover attractor already existed but only began to be sampled in 2007 and since, thanks to increasing internal variability.

3 Seasonal analysis

Our results may be sensitive to the fact that land masses mute variations in winter-spring ice area [18], whereas summer-autumn area is less affected. To address this we analyzed a derived index of 'equivalent sea-ice extent' [18], which is based on the latitude of the sea-ice edge where it is free to migrate, converted to an area, assuming there were no continents present. Fluctuations are much larger in this index, and recent summer-autumn ice retreats no longer stand out as anomalous [18], hence no recent bifurcation is detected (Supplementary Figure 7). However, there is still a signal of overall destabilization (Supplementary Figure 8), which appears before the signal in actual sea-ice area (Figure 3). This suggests our detection of a recent bifurcation in sea-ice cover could be (at least partly) a geographic property of the shrinkage of summer-autumn ice cover away from the continents facilitating larger fluctuations [18].

To examine whether this is the case, we looked at whether the new low ice cover state is just associated with summer-autumn intervals, by subdividing the original data (Figure 1a) into two composite series; summer-autumn (June-November inclusive) and winter-spring (December-May inclusive), removing the mean cycle from each, and re-running the analysis. Both subsets of the data carry part of the signal of the inferred bifurcation in 2007 (Supplementary Figure 9), suggesting the sampling of an alternative attractor is not a purely summer-autumn phenomenon. The signal is clearest in summer-autumn, but does not span as wide a range of window lengths as in the full data analysis. The summer-autumn (Supplementary Figure 10) and winter-spring (Supplementary Figure 11) data subsets also both show an overall rise in variance. However, only the summer-autumn data shows upward trends in the ACF and DFA indicators (Supplementary Figure 10). Thus, the recent signal of slowing down (i.e. destabilization) is associated primarily with summer-autumn sea-ice fluctuations.

4 Discussion

We present a conceptual model to try and explain recent sea-ice behavior in Figure 4, in which there is large seasonal forcing combined with a directional climate change forcing and stochastic variability. We hypothesize that combined effects of climate change and seasonal forcing pushed the system past a bifurcation point in the summer of 2007 and in every summer since, to a low ice cover state, but the strong seasonal reduction in forcing each winter caused the sea-ice to revert to its normal state.

The appearance of a new lower ice cover state is consistent with positive feedbacks between ice cover and other climate variables becoming stronger (because to separate two different stable states of a system under the same boundary conditions requires strong positive feedback). Several positive feedbacks have been identified in recent data. Sea-ice retreat since 1979 has exposed a dark ocean surface, causing 85% of the Arctic region to receive an increase in solar heat input at the surface, with an increase of 5% per year in some regions [22].

This is warming the upper Arctic ocean and contributing to melting on the bottom of the sea-ice [23]. Sea-ice retreat is also amplifying warming of the lower atmosphere in the Arctic [24], which is shifting precipitation from snow to rainfall, and where rain lands on the remaining sea ice cover, it is encouraging melt [25]. Finally, sea-ice loss is beginning to change atmospheric circulation patterns [26] (although how that feeds back to ice cover is unclear).

The bifurcation we detect clearly does not involve total seasonal sea-ice loss hence is sub-Arctic in scale. There is a precedent for this; past abrupt Arctic cooling and warming events have been linked to switches between alternative states for sea-ice cover in the Barents and Kara Seas region [27, 28]. Such sub-Arctic-scale switches can still have significant impacts, indeed recent ice loss from the Barents and Kara Seas has been linked to cold winter extremes over Eurasia [29].

The detected ongoing destabilization of the summer-autumn sea-ice cover suggests that a further bifurcation may be approaching. Either the new low ice cover state is a transient feature and the system may revert to the normal ice cover state. Or there could be a further abrupt decrease in summer-autumn ice cover.

5 Methods

5.1 Data and pre-processing

Sea-ice area takes into account the fraction of a grid cell (above 15%) that is covered by sea ice, and can be biased low, especially in summer when melt ponds are present. Sea-ice extent assumes that any grid point with more than 15% sea ice concentration is totally covered, hence it is biased high. Sea ice area data is from; http://arctic.atmos.uiuc.edu/cryosphere/timeseries.anom.1979-2008, as used on 'The Cryosphere Today' website. It spans 1979 to present at daily resolution (hence is already interpolated in places) and has the mean seasonal cycle over 1979-2008 removed (as is the standard convention). Sea ice extent data is from Eisenman [18]; ftp://ftp.agu.org/apend/gl/2010gl043741. It spans 1979-2009, and where it has 2-day resolution (1979 to mid-1987) or some minor gaps, we interpolate to daily resolution to obtain a homogeneous time-series, before removing the mean seasonal cycle over the entire dataset. The satellites and instruments used to compile these series are described by the National Snow and Ice Data Center; http://nsidc.org/.

5.2 Potential analysis

The time series are modelled by the stochastic differential equation:

$$\dot{z}(t) = -U'(z) + \sigma\eta, \tag{1}$$

where U is a polynomial potential of even order, η is a Gaussian white noise process of unit variance. Equation (1) has a corresponding Fokker-Planck equation

describing the probability density function, and crucially this has a stationary solution that depends only on the underlying potential function and the noise level, σ;

$$p(z) \sim \exp \frac{-2U(z)}{\sigma^2}. \tag{2}$$

This allows the underlying potential to be reconstructed from a kernel probability distribution of time-series data (and an estimate of the noise level) as:

$$U(z) = -\frac{\sigma^2}{2} \log p_d(z), \tag{3}$$

where p_d is the empirical probability density of the data.

We detect the order of the polynomial and hence the number of system states following the method in refs. [12, 13], plotting the results as a function of window length at the end of each sliding window in a colour contour plot (e.g. Figure 2b). The rate of correct detection depends on sliding window size [13]: when the window contains more than 400 data points, the success rate is 80%, even when noise level is up to five times bigger than the depth of the potential well; for larger windows it approaches 98%.

We derive the coefficients describing the shape of the potential using an unscented Kalman filter [12, 13], while we estimate the noise level using wavelet de-noising with Daubechies wavelets of 4th order (see ref. [13]).

The method assumes each subset of data is quasi-stationary and the noise is Gaussian white. For the 4-year intervals used to reconstruct the potentials in Figure 2c, the assumption of stationarity is reasonable. The noise in geophysical systems may be red rather than white, but the assumption of white noise can still be valid provided that the noise is stationary (DFA fluctuation exponent less than 1). By applying the potential model in such cases, we may attribute part of noise variability to the potential dynamics when analysing the two components of the potential model. This model is an approximation; still it allows us to derive accurately the structure of the potential for systems with stationary red noise. When there are no non-stationarities such noise cannot artificially create an additional system state.

5.3 Critical slowing down

Parabolic trends were removed prior to estimating two indicators (previously termed 'propagators' [15, 16]) of critical slowing down. This is because any trend affects autocorrelations and hence may cause false positive signals in the indicators. To test robustness we also performed an alternative pre-processing of data; first removing the quadratic downward trend and then deseasonalising the data, and obtained equivalent results.

5.4 ACF-indicator

Lag-1 autocorrelation was estimated [15, 16] by fitting an autoregressive model of order 1 (linear AR(1)-process) of the form:

$$z_{t+1} = c \cdot z_t + \sigma \eta_t, \tag{4}$$

where η_t is a Gaussian white noise process of unit variance, and the 'ACF-indicator' (AR1 coefficient):

$$c = e^{-\kappa \Delta t}, \tag{5}$$

where κ is the decay rate of perturbations, and $\kappa \to 0$ (i.e. $c \to 1$) as bifurcation is approached [15].

5.5 DFA-indicator

Detrended fluctuation analysis (DFA) extracts the fluctuation function of window size s, which increases as a power law if the data series is long-term power-law correlated:

$$F(s) \propto s^{\alpha} \tag{6}$$

where α is the DFA scaling exponent. In the short-term regime, as $c \to 1$ of the AR(1)-model, the slowing exponential decay is well approximated by a power law in which $\alpha \to 1.5$, in the time interval 10-100 units. Exponent α is rescaled, following ref. [16], to give a 'DFA-indicator' that reaches 1 at critical behavior.

5.6 Indicator trends

Upward trends in the indicators (rather than their absolute value) provide the primary early warning signal. The Kendall τ rank correlation coefficient [30] measures the strength of the tendency of an indicator to increase (positive values) or decrease (negative values) with time, against the null hypothesis of a random sequence of measurements against time (value approximately zero). As a sensitivity analysis, the sliding window along the time series was varied from 1/4 to 3/4 of the series length.

The research was supported by the NERC project 'Detecting and classifying bifurcations in the climate system' (NE/F005474/1) and by the AXA Research Fund through a postdoctoral fellowship for V.N.L. Research was carried out on the High Performance Computing Cluster at the University of East Anglia. We thank J. Imbers Quintana and A. Lopes for discussions and M. Scheffer for suggesting the conceptual model.

References

[1] Stroeve, J., Holland, M.M., Meier, W., Scambos, T., & Serreze, M., Arctic sea ice decline: Faster than forecast. *Geophysical Research Letters* 34, L09501 (2007).

[2] Nghiem, S.V. et al., Rapid reduction of Arctic perennial sea ice. *Geophysical Research Letters* 34, L19504 (2007).

[3] Boe, J., Hall, A., & Qu, X., September sea-ice cover in the Arctic Ocean projected to vanish by 2100. *Nature Geoscience* 2 (5), 341-343 (2009).

[4] Lenton, T.M. et al., Tipping Elements in the Earth's Climate System. *Proceedings of the National Academy of Sciences USA* 105 (6), 1786-1793 (2008).

[5] Lindsay, R.W. & Zhang, J., The Thinning of Arctic Sea Ice, 1988-2003: Have We Passed a Tipping Point? *Journal of Climate* 18, 4879-4894 (2005).

[6] Amstrup, S.C. et al., Greenhouse gas mitigation can reduce sea-ice loss and increase polar bear persistence. *Nature* 468 (7326), 955-958 (2010).

[7] Winton, M., Does the Arctic sea ice have a tipping point? *Geophysical Research Letters* 33 (23), L23504 (2006).

[8] Eisenman, I. & Wettlaufer, J.S., Nonlinear threshold behavior during the loss of Arctic sea ice. *Proceedings of the National Academy of Sciences USA* 106 (1), 28-32 (2009).

[9] Tietsche, S., Notz, D., Jungclaus, J.H., & Marotzke, J., Recovery mechanisms of Arctic summer sea ice. *Geophysical Research Letters* 38 (2), L02707 (2011).

[10] Notz, D., The future of ice sheets and sea ice: Between reversible retreat and unstoppable loss. *Proceedings of the National Academy of Sciences USA* 106, 20590-20595 (2009).

[11] Abbot, D.S., Silber, M., & Pierrehumbert, R.T., Bifurcations leading to summer Arctic sea ice loss. *Journal of Geophysical Research* 116, D19120 (2011).

[12] Livina, V.N., Kwasniok, F., & Lenton, T.M., Potential analysis reveals changing number of climate states during the last 60 kyr. *Climate of the Past* 6 (1), 77-82 (2010).

[13] Livina, V.N., Kwasniok, F., Lohmann, G., Kantelhardt, J.W., & Lenton, T.M., Changing climate states and stability: from Pliocene to present. *Climate Dynamics* 37 (11-12), 2437-2453 (2011).

[14] Scheffer, M. et al., Early warning signals for critical transitions. *Nature* 461, 53-59 (2009).

[15] Held, H. & Kleinen, T., Detection of climate system bifurcations by degenerate fingerprinting. *Geophysical Research Letters* 31, L23207 (2004).

[16] Livina, V.N. & Lenton, T.M., A modified method for detecting incipient bifurcations in a dynamical system. *Geophysical Research Letters* 34, L03712 (2007).

[17] Lenton, T.M., Early warning of climate tipping points. *Nature Climate Change* 1, 201-209 (2011).

[18] Eisenman, I., Geographic muting of changes in the Arctic sea ice cover. *Geophysical Research Letters* 37 (16), L16501 (2010).

[19] Livina, V.N., Ditlevsen, P.D., & Lenton, T.M., An independent test of methods of detecting and anticipating bifurcations in time-series data. *Physica A: Statistical Mechanics and its Applications*, doi:10.1016/j.physa.2011.1008.1025 (2011).

[20] Ditlevsen, P.D. & Johnsen, S.J., Tipping points: Early warning and wishful thinking. *Geophysical Research Letters* 37, L19703 (2010).

[21] Kinnard, C. et al., Reconstructed changes in Arctic sea ice over the past 1,450 years. *Nature* 479 (7374), 509-512 (2011).

[22] Perovich, D.K. et al., Increasing solar heating of the Arctic Ocean and adjacent seas, 1979-2005: Attribution and role in the ice-albedo feedback. *Geophysical Research Letters* 34, L19505 (2007).

[23] Perovich, D.K., Richter-Menge, J.A., Jones, K.F., & Light, B., Sunlight, water, and ice: Extreme Arctic sea ice melt during the summer of 2007. *Geophysical Research Letters* 35, L11501 (2008).

[24] Screen, J.A. & Simmonds, I., The central role of diminishing sea ice in recent Arctic temperature amplification. *Nature* 464 (7293), 1334-1337 (2010).

[25] Screen, J. & Simmonds, I., Declining summer snowfall in the Arctic: causes, impacts and feedbacks. *Climate Dynamics*, 10.1007/s00382-00011-01105-00382 (2011).

[26] Overland, J.E. & Wang, M., Large-scale atmospheric circulation changes are associated with the recent loss of Arctic sea ice. *Tellus* A 62 (1), 1-9 (2010).

[27] Bengtsson, L., Semenov, V.A., & Johannessen, O.M., The Early Twentieth-Century Warming in the Arctic - A Possible Mechanism. *Journal of Climate* 17 (20), 4045-4057 (2004).

[28] Semenov, V.A., Park, W., & Latif, M., Barents Sea inflow shutdown: A new mechanism for rapid climate changes. *Geophysical Research Letters* 36 (14), L14709 (2009).

[29] Petoukhov, V. & Semenov, V.A., A link between reduced Barents-Kara sea ice and cold winter extremes over northern continents. *J. Geophys. Res.* 115 (D21), D21111 (2010).

[30] Kendall, M.G., *Rank Correlation Methods.* (Charles Griffin & Company Limited, London, 1948).

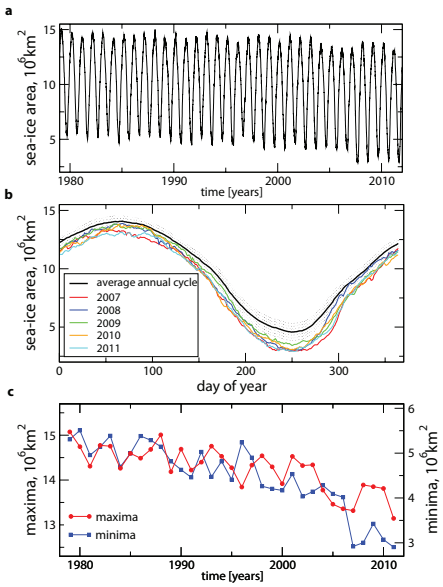

Figure 1: Arctic sea-ice area from satellite data. (a) Arctic sea-ice area. (b) The mean annual cycle of the area data over 1979-2008 inclusive (solid line, shaded area denotes two error bars), together with the last five anomalous years. (c) Annual maxima (left axis) and minima (right axis) showing an abrupt increase in amplitude of the seasonal cycle in 2007.

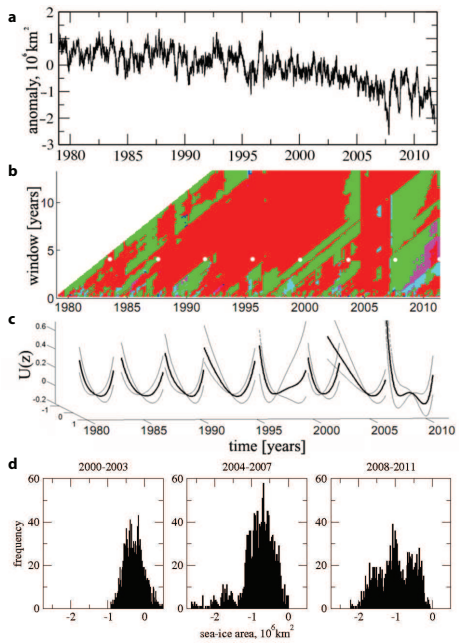

Figure 2: Detection of a bifurcation in Arctic sea-ice area. (a) Sea-ice area anomaly, daily data with mean seasonal cycle removed. (b) Contour plot of number of detected states, where red = 1 detected state, green = 2, cyan = 3, magenta = 4. Results plotted as a function of sliding window length at the end of the window. (c) Reconstructed potential curves of eight 4-year time intervals, corresponding to the white dots in (b). Here 'z' is sea-ice area fluctuation on a shifted scale. Faint lines are potential curves derived from error estimates on the coefficients of the polynomial potential function (for details see ref. 11). In the penultimate interval 2004-2007 a second state starts to appear and in the final interval 2008-2011 there are two states of comparable stability. (d) Histograms of the data for 2000-2003, 2004-2007, 2008-2011 from which the corresponding potential curves are derived (see Methods).

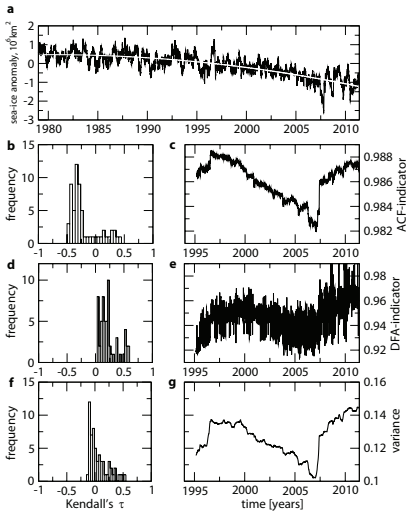

Figure 3: Search for early warning signals of bifurcation in Arctic sea-ice area data. (a) Sea-ice area anomaly (as in Figure 2a) showing the quadratic downward trend that is removed prior to calculating the instability indicators. Right panels show example indicators using a sliding window of length half the series, with results plotted at the end of the sliding window. Indicators from: (c) autocorrelation function (ACF), (e) detrended fluctuation analysis (DFA) and (g) variance. Left panels show histograms of the Kendall statistic for the trend in the indicators when varying the sliding window length from 1/4 to 3/4 of the series: (b) ACF-indicator, (d) DFA-indicator, (f) variance.

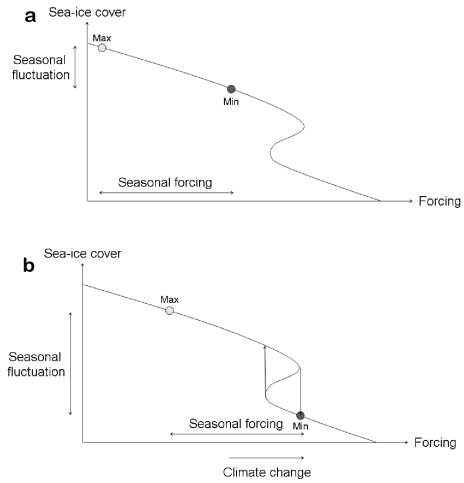

Figure 4: Schematic model of sea-ice dynamics with changes exaggerated: (a) before bifurcation, showing range of seasonal forcing and seasonal response of normal ice cover state, and (b) after climate change forcing, the system passes a bifurcation in summer to an alternative lower ice cover state, but reverts later in the season to the normal ice cover state.